

A Study of the Reaction $\text{Li} + \text{O}_2 + \text{M}$ ($\text{M} = \text{N}_2, \text{He}$) over the Temperature Range 267–1100 K by Time-Resolved Laser-Induced Fluorescence of $\text{Li}(2^2\text{P}_J - 2^2\text{S}_{1/2})$

John M. C. Plane* and B. Rajasekhar

Rosenstiel School of Marine and Atmospheric Science, University of Miami, Miami, Florida 33149
(Received: November 30, 1987)

We present an investigation of the recombination reaction between lithium atoms and O_2 in the presence of both N_2 and He as bath gases. Lithium atoms were produced by the pulsed photolysis of either LiI , LiOH , or LiO_2 molecules in the presence of an excess of O_2 and the bath gas. The Li atom concentration was then monitored by laser-induced fluorescence of the metal atoms at $\lambda = 670.7$ nm using a pulsed nitrogen-pumped dye laser and boxcar integration of the fluorescence signal. Termolecular behavior was demonstrated in the case of both bath gases, and absolute third-order rate constants were obtained over the temperature range 267–1100 K. A fit of these data to the form AT^{-n} yields $k(\text{M} = \text{N}_2) = (4.30 \pm 1.36) \times 10^{-30}(T/300 \text{ K})^{-(1.02 \pm 0.06)} \text{ cm}^6 \text{ molecule}^{-2} \text{ s}^{-1}$ and $k(\text{M} = \text{He}) = (1.25 \pm 0.48) \times 10^{-30}(T/300 \text{ K})^{-(0.38 \pm 0.08)} \text{ cm}^6 \text{ molecule}^{-2} \text{ s}^{-1}$. It is demonstrated that these measurements are essentially in the low-pressure limit; the rate coefficients are then extrapolated from the experimental temperature range to ambient mesospheric temperatures ($140 \text{ K} < T < 240 \text{ K}$) and to flame temperatures ($1500 \text{ K} < T < 2200 \text{ K}$) by means of a satisfactory fit to the Troe formalism.

Introduction

The recombination reaction between lithium atoms and oxygen



is of great theoretical and applied interest. The reaction involves the association of two neutral fragments to form LiO_2 which is known to exist as an ion pair, Li^+O_2^- ; evidence for this comes from IR spectroscopic measurements of Li and O_2 coadsorbed onto an inert gas matrix.¹ This study¹ showed that the LiO_2 molecule exists in an isosceles triangular (C_{2v}) configuration and that the Li 2s electron is almost completely transferred into the 3π antibonding orbital of O_2 . This observation was supported by a subsequent theoretical study of the nature of the ground $2^2\text{A}''$ state of the molecule.² The recombination reaction between Li and O_2 thus involves a crossing from a long-range covalent attractive surface onto a close-range ionic potential surface, estimated to occur at an internuclear separation of 2.95 \AA .² We have previously discussed the effects of this type of covalent/ionic curve crossing on the rates of recombination reactions of the type alkali metal + OH + He,³ alkali metal + I + He,⁴ and Na, K + O_2 + M.⁵ In essence, the fairly large bond energies and very low vibrational frequencies associated with the Coulombic nature of the ionic potential surface lead to recombination rates of reactions involving alkali-metal atoms which are enhanced by orders of magnitude relative to the analogous reactions of, for example, H atoms.³⁻⁵

A primary motivation for the present work is to gain an understanding of the chemistry of lithium in the mesosphere, the region of the earth's atmosphere which couples the ionosphere and stratosphere. The major source of Li is considered to be meteoritic in origin,⁶ although injections of Li from the lower atmosphere both by atomic bombs⁷ and volcanic eruptions⁸ have

been observed. Metallic elements which are ablated from meteors entering the earth's atmosphere play a significant role in the structure of the D and E regions of the upper atmosphere.^{9,10} A layer of atomic Li has been observed at about 90 km by using spectrophotometric measurements of twilight resonance emissions¹¹ and also by LIDAR (laser radar).¹² By analogy with recent models proposed to describe the chemistry of Na and K in the upper atmosphere,¹³⁻¹⁵ LiO_2 can be expected to be a major sink for atomic Li, perhaps limited during the day by direct photolysis and at nighttime by reaction with ambient O and H atoms. Of particular interest is to understand the large winter enhancement in the Li atom concentration at 90 km at high latitudes, relative to that of Na or K.¹¹ This tenfold seasonal variation in Li may be related to the large seasonal changes in the bulk gas concentration and temperature which occur at high latitudes (e.g., 140 K in summer to 230 K in winter at 70° N in the mesosphere¹⁶). An important objective of this study is thus to measure the absolute value and temperature dependence of $k_1(T, \text{M} = \text{N}_2)$ as close to mesospheric temperatures as possible.

A second important application of the results of the present study is in modeling the combustion chemistry of lithium. In particular, the Li/Na ratio technique has been established as an important method for determining the hydrogen atom concentration in the afterburn region of a flame.¹⁷⁻²⁰ The method relies on the assumption that the concentrations of Li and LiOH are in equilibrium through the balanced conversion reactions involving H_2O and H.²¹ We have shown recently,⁵ along with other workers,^{22,23} that the recombination reactions between Na or K

(1) Andrews, L. *J. Chem. Phys.* **1969**, *50*, 4288. Hatzenbuehler, D. A.; Andrews, L. *Ibid.* **1972**, *56*, 3398.

(2) Alexander, M. H. *J. Chem. Phys.* **1978**, *69*, 3502.

(3) Husain, D.; Plane, J. M. C.; Chen, C. X. *J. Chem. Soc., Faraday Trans. 2* **1984**, *80*, 1465, 1619; **1985**, *81*, 561, 769.

(4) Husain, D.; Plane, J. M. C.; Chen, C. X. *J. Chem. Soc., Faraday Trans. 2* **1985**, *81*, 1675. Plane, J. M. C.; Husain, D. *J. Phys. Chem.* **1986**, *90*, 501. Plane, J. M. C.; Husain, D. *J. Chem. Soc., Faraday Trans. 2* **1986**, *82*, 897.

(5) Husain, D.; Plane, J. M. C. *J. Chem. Soc., Faraday Trans. 2* **1982**, *78*, 163, 1175. Husain, D.; Marshall, P.; Plane, J. M. C. *Ibid.* **1985**, *81*, 301; *J. Photochem.* **1986**, *32*, 1.

(6) Goldberg, R. A.; Aikin, A. C. *Science* **1973**, *180*, 294.

(7) Sullivan, H. M.; Hunte, D. M. *Can. J. Phys.* **1964**, *42*, 937.

(8) Gadsden, M. *Proceedings of the Royal Meteorological Society Specialist Group in Atmospheric Chemistry, at Hertford College, Oxford, April 6, 1983*.

(9) Murad, E. *J. Geophys. Res.* **1978**, *83*, 5525.

(10) Brown, T. L. *Chem. Rev.* **1973**, *73*, 645.

(11) Henriksen, K.; Sivjee, G. G.; Deehr, C. S. *J. Geophys. Res.* **1980**, *85*, 5153. Henriksen, K.; Deehr, C. S.; Sivjee, G. G.; Myrabo, H. K. *J. Atmos. Terr. Phys.* **1986**, *48*, 159.

(12) Jegou, J.-P.; Chanin, M.-L.; Megie, G.; Blamont, J. E. *Geophys. Res. Lett.* **1980**, *7*, 995.

(13) Liu, S. C.; Reid, G. C. *Geophys. Res. Lett.* **1979**, *6*, 283.

(14) Thomas, L.; Isherwood, M. C.; Bowman, M. R. *J. Atmos. Terr. Phys.* **1983**, *45*, 587.

(15) Swider, W. J. *Geophys. Res.* **1987**, *92*, 5621.

(16) Brasseur, G.; Solomon, S. *Aeronomy of the Middle Atmosphere*; Reidel: Dordrecht, 1986.

(17) Bulewicz, E. M.; James, C. G.; Sugden, T. M. *Proc. R. Soc. London, Ser. A* **1956**, *235*, 89.

(18) McEwan, M. J.; Phillips, L. F. *Combust. Flame* **1965**, *9*, 420; **1967**, *11*, 63.

(19) Muller, C. H.; Schofield, K.; Steinberg, M. *J. Chem. Phys.* **1980**, *72*, 6620.

(20) Jensen, D.; Jones, G. A.; Mace, A. C. H. *J. Chem. Soc., Faraday Trans. 1* **1979**, *75*, 2377. Jensen, D. E.; Jones, G. A. *Ibid.* **1982**, *78*, 2843.

(21) Plane, J. M. C.; Rajasekhar, B. *J. Chem. Soc., Faraday Trans. 2*, **1988**, *84*, 273.

and O₂ are rapid at high temperatures and that large production fluxes of the superoxides in oxygen-rich flames will occur. The superoxides are then expected to undergo thermal dissociation^{24,25} or to be converted to the more thermally stable hydroxide through fast reactions with radicals such as H atoms in the flame.²⁵ A calculation of the Li–O₂ bond energy² indicates that LiO₂ is much more stable than the lower alkali-metal superoxides. It will thus be less prone to thermal dissociation, and provided that $k_1(T > 1500 \text{ K})$ is fast enough, the enhanced production of LiOH may significantly perturb the Li/LiOH balance in the flame. Thus, the Li/LiOH distribution may not be equilibrated except at high temperatures and in fuel-rich flames,²⁵ and the Li/Na method for determining H atom concentrations may be subject to significant error. We have recently carried out a study on the reaction between Li and H₂O.²¹ The present study thus represents a further step in producing a better characterization of the Li/Na technique by measuring $k_1(T, M = \text{N}_2)$ at the highest temperatures that are possible experimentally and then extrapolating to flame conditions.

Kramer et al.²⁶ have investigated reaction 1 by the technique of laser photolysis of LiI vapor followed by detection of the resulting Li atoms by resonance ionization spectroscopy (RIS). Two third-order rate coefficients were measured, namely, $k_1(M = \text{He}, T = 460 \text{ K})$ and $k_1(M = \text{Ar}, T = 390 \text{ K})$. However, those investigators²⁶ did not determine the temperature dependence of these reactions nor study reaction 1 with N₂ as a third body, both of which are pertinent to characterizing the chemistry of Li in the upper atmosphere and in flames.

Experimental Section

Reaction 1 was investigated by using the technique of time-resolved laser-induced fluorescence spectroscopy of Li atoms at 670.7 nm (Li(2²P_{1/2})–Li(2²S_{1/2})), following the pulsed photolysis of lithium salt vapor in an excess of O₂ and N₂ or He bath gas. The experimental system is described in detail elsewhere,^{21,27,28} and here we give a brief description except where emphasizing changes in the experimental arrangement for carrying out the present work.

The stainless steel reactor consists of a central cylindrical reaction chamber at the intersection of two sets of arms which cross orthogonally. One pair of opposite arms provide the optical coupling for the nitrogen-pumped dye laser (Laser Science Inc., Model VSL-337; laser dye DCM, maximum output 15 μJ) which is used to probe Li atoms in the central chamber. The photolyzing flash lamp (EG&G, Model FX193U, maximum flash energy 7 J) is coupled to the central chamber through a pair of Suprasil lenses and through a side arm either orthogonal to the laser^{27,28} or opposite the laser so that the flash lamp and laser are collinear.²¹ Of the pair of side arms orthogonal to the laser, one side arm is independently heated and is used to provide the source of the photolytic precursor of Li atoms, hereafter referred to as the heat pipe; the other side arm provides an exit for the gas flows from the central chamber to the pump. In the present study, three different precursors were used. Most work was performed using LiI, which is both relatively volatile²⁹ and has a large photolysis cross section.³⁰ LiI was placed in a tantalum boat in the heat pipe and then heated to about 850 K, where the concentration

of LiI vapor in equilibrium above the molten salt is 1.8×10^{15} molecules cm⁻³.²⁹ The vapor is then entrained in a flow of the bath gas and carried into the central chamber. LiI was the precursor used in all the low-temperature studies where there is a major loss of Li salt vapor in the central chamber through deposition onto the cool walls; in this case the laser and flash lamp were configured orthogonally since this arrangement is optimal for reducing the scattered laser light signal when sensitive detection of Li atoms is at a premium.

For reasons discussed in the next section, experiments at high temperatures were also carried out using LiOH and LiO₂ as Li atom precursors. When either of these precursors is used, the laser and flash lamp beams were arranged to be collinear.²¹ LiOH vapor was generated by placing a sample of powdered LiOH in the tantalum boat in the heat pipe. However, in this case the temperature of the boat must be accurately controlled at about 820 K,²¹ not only to generate a sufficient vapor pressure of LiOH (5.4×10^{11} molecules cm⁻³ in equilibrium above the liquid hydroxide in the boat²⁹) but also to prevent the rapid decomposition of LiOH at higher temperatures.²¹ In order to achieve this, the boat was supported on a chromel–alumel thermocouple which entered the arm through a cooled vacuum coupling.²¹ LiO₂ as a precursor was made in situ in the reactor: a flow of pure Li vapor from the heat pipe was mixed with a flow of excess O₂ in the central chamber to form LiO₂ by reaction 1. In this case, a spiral wick of stainless steel mesh (gauge 150) was inserted into the heat pipe which was then run first in the heat pipe oven mode^{3,4,31} to purify the sample of Li metal before conducting kinetic runs.

The central chamber is enclosed in a furnace which can heat it to over 1200 K. Alternatively, the furnace can be filled with powdered “dry ice” to cool the chamber from room temperature down to about 260 K when the heat pipe is running at over 800 K. The temperature of the gases flowing through the chamber is monitored by a chromel–alumel thermocouple that is permanently inserted into the chamber slightly below the height at which the flash lamp and laser beams pass through it.

The laser-induced fluorescence signal is monitored vertically above the central chamber by a photomultiplier tube (Thorn EMI Gencom Inc., Model 9816QB) after passing through an interference filter centered at 670 nm (Oriol Corp., fwhm = 10 nm) to exclude scattered light from the flash lamp. The PMT is cooled to below 25 °C by a flow of chilled air and is coupled to the central chamber by a vertical side arm above the chamber. This side arm, the heat pipe, and the pair of opposite arms coupling the laser to the central chamber each feature an input for a gas flow which enters the side arm and then flows into the central chamber. These flows sweep the cooled end windows on the three side arms clear of Li salt vapor from the central chamber. Taking the examples of LiI as the precursor and N₂ as the bath gas, the flows consist of a three-way split of a main flow of O₂/N₂ from the gas-handling line into the reactor. The ratio of O₂ to N₂ in this flow is varied by mixing a flow of a stock mixture of O₂/N₂ with one of pure N₂ to give a combined flow of 50 sccm. The flow of LiI/N₂ from the heat pipe is kept constant at 50 sccm. The central chamber thus provides a mixing vessel for the flows of LiI/N₂ and O₂/N₂. The size of the flows and the reactor design are such that oxygen from the central chamber does not mix into the heat pipe. The total pressure in the reactor is controlled by a needle valve on the exit line to the pump.

When working near or below room temperature, it became essential to shorten the residence time of the gas mixture in the central chamber in order to limit the loss of LiI vapor onto the cool reactor walls. This was achieved by increasing the mass flow rates and working at lower total pressures. A simple diffusion calculation²⁷ indicates that, at a total mass flow rate of 100 sccm through the central chamber, less than 0.005% of the LiI vapor from the heat pipe will reach the photolysis region in the center. In some experiments the total flow rate was doubled to 200 sccm and the pressure in the reactor lowered to 10 Torr. The estimated residence time of the gas in the central chamber is then about

(22) Husain, D.; Lee, Y. H.; Marshall, P. *Combust. Flame* **1987**, *68*, 143.

(23) Silver, J. A.; Zahniser, M. S.; Stanton, A. C.; Kolb, C. E. In *Proceedings of the 20th International Symposium on Combustion*; The Combustion Institute: Pittsburgh, PA, 1984; p 605.

(24) Jensen, D. E. *J. Chem. Soc., Faraday Trans. 1* **1982**, *78*, 2835.

(25) Hynes, A. J.; Steinberg, M.; Schofield, K. *J. Chem. Phys.* **1984**, *80*, 2585.

(26) Kramer, S. D.; Lehmann, B. E.; Hurst, G. S.; Payne, M. G.; Young, J. P. *J. Chem. Phys.* **1982**, *76*, 3614.

(27) Plane, J. M. C. *J. Phys. Chem.* **1987**, *91*, 6552.

(28) Plane, J. M. C.; Saltzman, E. S. *J. Chem. Phys.* **1987**, *87*, 4606.

(29) *JANAF Thermochemical Tables*, 3rd ed.; Chase, Jr., M. W., Davies, C. A., Downey, Jr., J. R., Frurip, D. J., McDonald, R. A., Syverud, A. N., Eds. *J. Phys. Chem. Ref. Data* **1985**, *14*.

(30) Brodhead, D. C.; Davidovits, P.; Edelstein, S. A. *J. Chem. Phys.* **1969**, *51*, 3601.

(31) Vidal, C. R.; Cooper, J. J. *J. Appl. Phys.* **1969**, *40*, 3370.

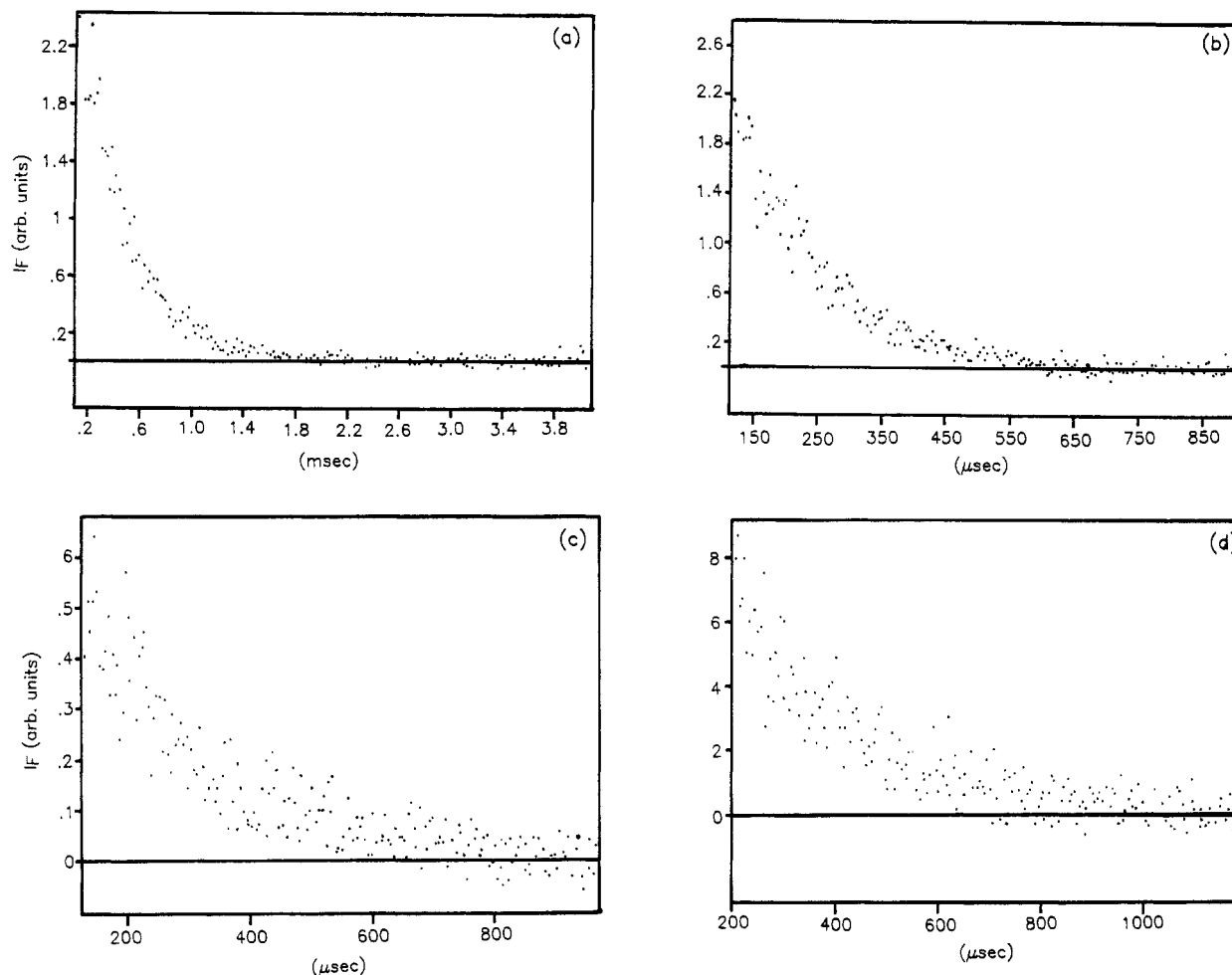


Figure 1. Time-resolved decay of the LIF signal from Li atoms at $\lambda = 670.7$ nm ($\text{Li}(2^2P_J) - \text{Li}(2^2S_{1/2})$) following the pulsed photolysis of LiI vapor at $T = 267$ K: (a) $[\text{O}_2] = 1.5 \times 10^{15}$ molecules cm^{-3} , $[\text{N}_2] = 3.6 \times 10^{17}$ molecules cm^{-3} ; (b) $[\text{O}_2] = 4.5 \times 10^{15}$ molecules cm^{-3} , $[\text{N}_2] = 3.6 \times 10^{17}$ molecules cm^{-3} ; (c) $[\text{O}_2] = 1.1 \times 10^{15}$ molecules cm^{-3} , $[\text{N}_2] = 5.4 \times 10^{17}$ molecules cm^{-3} ; (d) $[\text{O}_2] = 4.3 \times 10^{15}$ molecules cm^{-3} , $[\text{He}] = 5.4 \times 10^{17}$ atoms cm^{-3} .

1 s. By verifying that the measured decay rate of the LIF signal was not a function of the residence time, which was varied by altering the total mass flow rate while keeping the total reactor pressure constant, it was ascertained that complete mixing of the flows in the central chamber occurred when working with these reduced residence times. This is in accord with the estimated average diffusion distance of a gas molecule during its residence in the central chamber being about twice the dimensions of the chamber.³²

The experimental system is controlled by a pulse/delay generator (Stanford Research Systems, SRS DG535). In each triggering sequence, the PMT is first gated for 60 μs to reduce its gain while the flash lamp is fired. The flash lamp and the boxcar averager (Stanford Research Systems, Model SR250) are triggered simultaneously 14 μs after the PMT is gated. The probe laser pulse is triggered by the boxcar to coincide with the opening of the integrator gate as it is scanned to monitor the LIF signal at increasing time intervals after the flash lamp fires. Data collection was normally initiated about 105 μs after the flash lamp is fired.²⁷ Each scan is divided into 200 bins, and the scans were generally repeated once and averaged to improve the signal-to-noise ratio. The averaged decays were then transferred to a microcomputer for a curve-fitting analysis and storage.

Materials. Oxygen (99.995% purity, Liquid Carbonic) was trapped at 97 K before use. Nitrogen (99.999%, Liquid Carbonic) and helium (99.9999%, Matheson "Matheson Purity") were used without further purification. LiI (99%, Aldrich, Anhydrous) and LiOH monohydrate (99%, Sigma Chemical Co.) were refluxed

in the side arm at 700–850 K for several hours prior to kinetic experiments to remove I_2 and H_2O , respectively. Li metal wire (99.9%, Aesar/Johnson Matthey) was cleaned with solvent and then refluxed in the heat pipe oven for several hours before use.

Results

Figure 1 illustrates examples of the decay of the LIF signal at $\lambda = 670.7$ nm ($\text{Li}(2^2P_J) - \text{Li}(2^2S_{1/2})$), generated by the pulsed photolysis of LiI in the presence of O_2 and N_2 or He at $T = 267$ K. These decays, being recorded at the lowest temperature investigated in the present series of experiments, generally exhibit the worst signal-to-noise ratio because of the loss of the LiI precursor through deposition on the walls. The figure is included in order to demonstrate that the signal-to-noise ratio was nevertheless adequate for the curve-fitting procedure described below. Inspection of the four parts of Figure 1 indicates that the decay rate increases with both $[\text{O}_2]$ and $[\text{N}_2]$ and that the decay rate is much faster in the presence of N_2 than He as a bath gas.

Previous experience with this experimental system²¹ has shown that the quality of signal illustrated in Figure 1 corresponds to the concentration of Li atoms produced in the flash being on the order of about 10^9 atoms cm^{-3} ; this is about a factor of 10^6 less than the concentrations of O_2 employed. When working at temperatures above 800 K in the central reaction chamber, the concentration of LiI entering the central chamber was restricted by running the temperature of the LiI source in the heat pipe below 800 K, and the flash lamp energy was turned down below 1 J to limit the photolytic production of Li atoms. Thus, the decay of Li atoms due to reaction 1 (and from diffusion out of the center of the reactor) was under pseudo-first-order conditions and was exponential in form. We have shown previously^{27,28} that expo-

(32) Atkins, P. W. *Physical Chemistry*; Oxford University Press: Oxford, 1978.

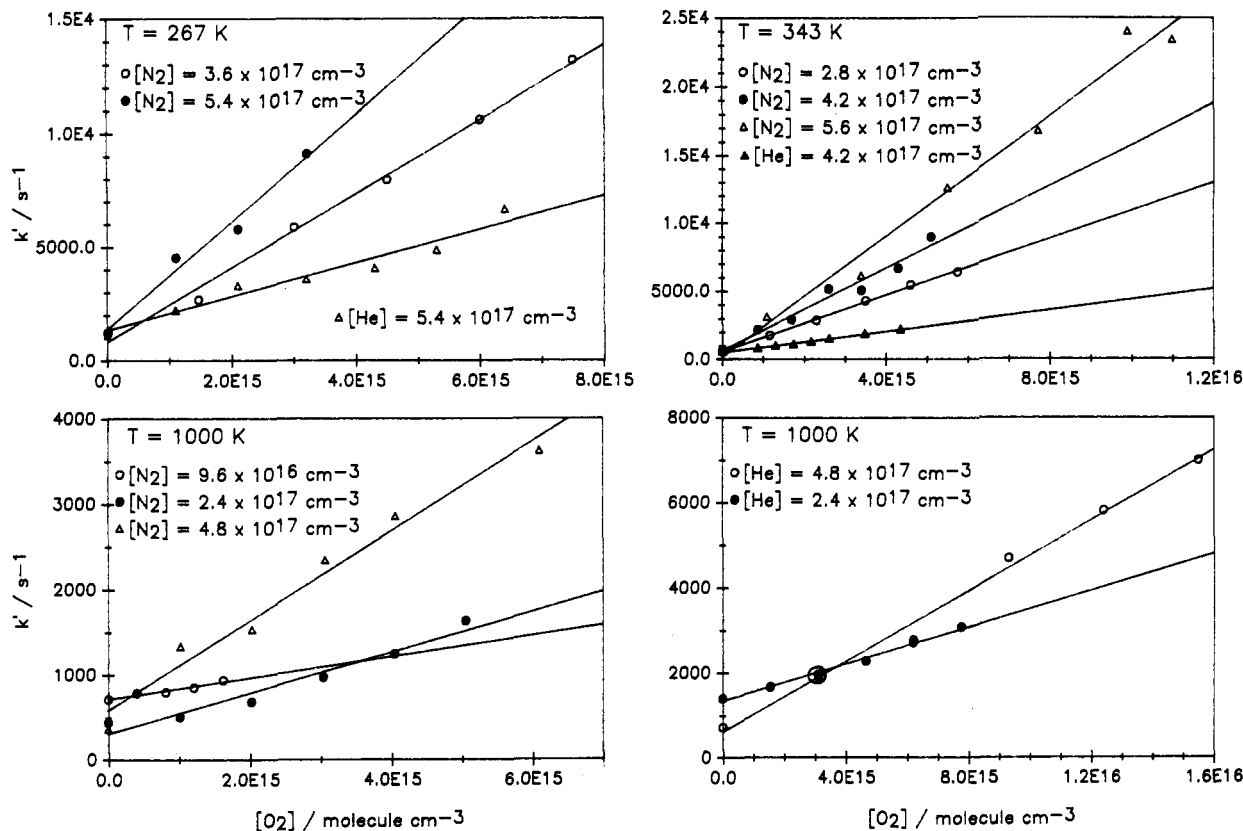


Figure 2. Plots of k' against $[\text{O}_2]$ at constant $[\text{N}_2]$ or $[\text{He}]$, for $T = 267, 343,$ and 1000 K . The solid lines are linear regression curves through the data.

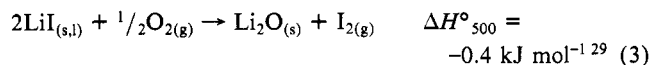
nential decays of the signal-to-noise quality in Figure 1 can be fitted satisfactorily to the form $A \exp(-k't)$, where k' is given by

$$k' = k_{\text{diff}} + k_1[\text{O}_2][\text{M}] \quad (2)$$

The term k_{diff} describes diffusion of the Li atoms out of the volume formed by the intersection of the flash lamp beam passing through the central chamber of the reactor, the laser beam, and the field of view of the PMT. The analysis of this term to obtain diffusion coefficients for Li atoms in He and N_2 has been described previously.^{21,27} The present measurements of k' in the absence of O_2 are in good accord with those measurements,^{21,27} even at the lowest temperatures studied when any kinetic effects due to the presence of LiI dimers²⁹ and clusters will be greatest.

Experiments were carried out over the temperature range 267–1100 K for $\text{M} = \text{N}_2$ and $T = 267$ –1000 K for $\text{M} = \text{He}$. The lower temperature limit is governed by the constraint of generating a sufficient concentration of LiI vapor in the reaction vessel to produce a detectable concentration of Li atoms upon photolysis; this limit is prescribed by the heat-transfer balance between the flow of hot gas from the heat pipe at $T = 850 \text{ K}$ and the powdered "dry ice" packing around the central chamber. The upper limit is constrained by the physical design of the reactor.²⁷

Under some conditions we observed a large production of I_2 when a flow of O_2 was switched on through the central chamber. This occurred when the chamber was heated to temperatures above about 500 K and immediately after distilling a fresh sample of LiI in the heat pipe in order to purify it. Since the rate constant of the reaction between Li and I_2 is probably at least as fast as their collision frequency,³³ this represented a serious artifact. We believe that the reaction producing I_2 is heterogeneous:



The alternative gas-phase reaction between LiI dimers and O_2 to produce I_2 is thermodynamically unfavorable.²⁹ Reaction 3 is thermodynamically favorable because of the very stable nature

of Li_2O .²⁹ The evidence for the heterogeneity arises from the observation that after running the reactor with the flows on for several hours the production of I_2 becomes much slower. We presume that during the initial distillation procedure to purify LiI in the boat, which was carried out under a pure N_2 blanket, the central chamber received a coating of LiI from the heat pipe. When a flow of O_2/N_2 was then switched on to begin a kinetic experiment, this hot coating of LiI reacted with O_2 according to reaction 3 and was converted to Li_2O . After this occurred the rate of deposition of new LiI from the heat pipe onto the chamber walls during the kinetic experiments was too small to produce a significant quantity of I_2 , and when the central chamber was heated to temperatures at or above 800 K, no effect from the presence of I_2 on the kinetic measurements was observed (see below). Presumably, this is because there will be less of a tendency for LiI vapor to condense on the chamber walls at high temperature; furthermore, any I_2 that is produced will be overwhelmingly dissociated into the atomic form.²⁹ When working below 500 K, even with a newly distilled sample of LiI in the heat pipe, there was very little evidence of I_2 production, presumably because reaction 3 is too slow.

The problem with I_2 production in the reactor thus prevented measurements of $k_1(T)$ between 500 and 800 K. Bearing in mind the applications of the present study to atmospheric and combustion processes, this is not a serious limitation. In order to verify that the high-temperature measurements were indeed not being affected by I_2 production, we conducted some of the high-temperature experiments at $T = 900 \text{ K}$ using LiOH and LiO_2 as precursors of Li atoms (see Experimental Section). We observed no significant difference in the Li atom decay rates when the experiments were then repeated with LiI for the same $[\text{O}_2]$ and $[\text{M}]$.

Equation 2 implies that the term k_{diff} should comprise the intercept of a plot of k' against $[\text{O}_2]$. Such plots are illustrated in Figure 2, for the temperatures 267, 343, and 1000 K. k' exhibits a clear linear dependence on $[\text{O}_2]$ and a dependence on $[\text{N}_2]$ or $[\text{He}]$. Reaction 1 is clearly much slower in the presence of He. The slopes of these plots are obtained from a linear regression

(33) Edelman, S. A.; Davidovits, P. *J. Chem. Phys.* 1971, 55, 5164.

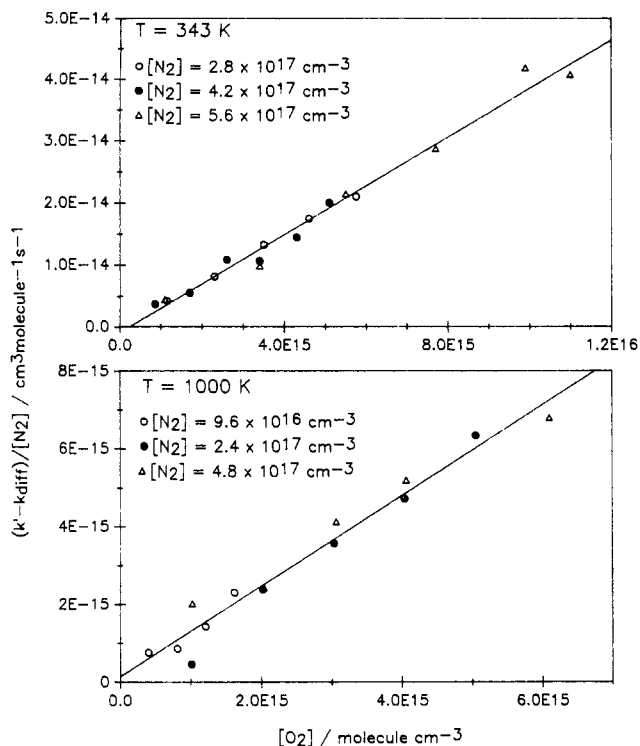


Figure 3. Plots of $(k' - k_{\text{diff}})/[\text{N}_2]$ against $[\text{O}_2]$ for $T = 343$ and 1000 K. The solid lines are linear regression curves through the data.

TABLE I: Experimental Determinations of $k_1(\text{Li} + \text{O}_2 + \text{M})$ as a Function of T (Quoted Uncertainty is 2σ)

T/K	$k_1/(10^{-30} \text{ cm}^6 \text{ molecule}^{-2} \text{ s}^{-1})$	press./Torr	T/K	$k_1/(10^{-30} \text{ cm}^6 \text{ molecule}^{-2} \text{ s}^{-1})$	press./Torr
M = N₂					
267	4.5 ± 0.4	10-15	500	2.6 ± 0.3	10
298	3.9 ± 0.4	10-15	900	1.4 ± 0.2	25-50
343	3.7 ± 0.3	10-20	1000	1.2 ± 0.1	10-50
400	3.1 ± 0.2	10	1100	0.92 ± 0.15	25-50
M = He					
267	1.4 ± 0.2	15-25	500	1.0 ± 0.1	25-50
285	1.3 ± 0.2	20	800	0.91 ± 0.12	25-100
330	1.1 ± 0.1	40	900	0.75 ± 0.11	25-100
343	1.1 ± 0.1	20	1000	0.83 ± 0.12	25-50
353	1.2 ± 0.2	12-20			

calculation, and the fitted curves are shown in Figure 2. Parts a and b of Figure 3 are plots of $(k' - k_{\text{diff}})/[\text{N}_2]$ against $[\text{O}_2]$ using the data (for $\text{M} = \text{N}_2$) in Figures 2, b and c, respectively, demonstrating that reaction 1 is also directly proportional to the concentration of the third body. Linear regression calculations of the slopes of Figure 3a,b thus yield estimates of k_1 . Note that within experimental error the intercepts pass through the origin, establishing the simple kinetic nature of the system described by eq 2. Table I contains a list of the measured values of k_1 as a function of temperature for both N_2 and He as third bodies. The quoted errors represent the expected 2σ errors from the linear regression fit to each plot. Included in Table I is the pressure range (Torr) over which measurements were carried out at a particular temperature.

Figure 4 displays the data contained in Table I, plotted as $\ln k$ vs $\ln T$. A linear regression fit weighted by the uncertainties in Table I yields

$$k_1(T, \text{M} = \text{N}_2) = (4.30 \pm 1.36) \times 10^{-30} (T/300 \text{ K})^{-(1.02 \pm 0.06)} \text{ cm}^6 \text{ molecule}^{-2} \text{ s}^{-1}$$

$$k_1(T, \text{M} = \text{He}) = (1.25 \pm 0.48) \times 10^{-30} (T/300 \text{ K})^{-(0.38 \pm 0.08)} \text{ cm}^6 \text{ molecule}^{-2} \text{ s}^{-1} \quad (4)$$

The quoted error limits are the expected 2σ uncertainties calcu-

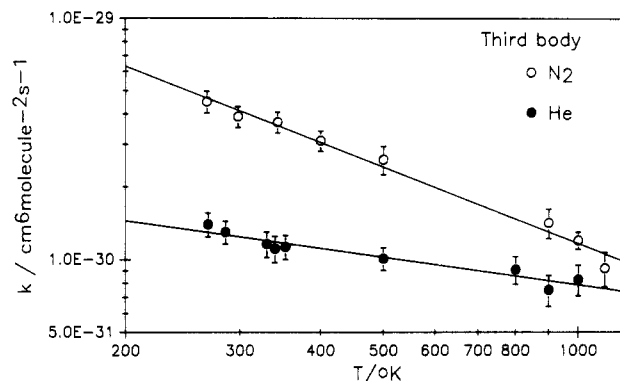


Figure 4. Plots of $\ln k$ against $\ln T$ for $\text{M} = \text{N}_2$ and He. The solid lines are weighted linear regression curves through the experimental data for each third body.

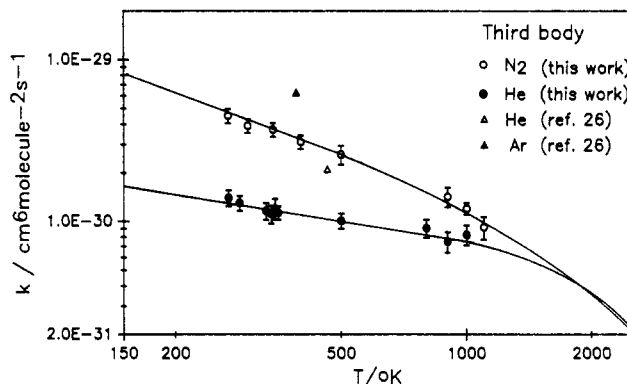


Figure 5. Plots of all experimental data on the reaction $\text{Li} + \text{O}_2 + \text{M}$, where $\text{M} = \text{He}, \text{N}_2$, and Ar. The solid lines are extrapolations of the experimental data from the present work from $T = 150$ to 2000 K using the Troe formalism.

lated from the absolute errors in Table I and depicted in Figure 4.

Discussion

To the best of our knowledge, this is the first kinetic investigation of the reaction $\text{Li} + \text{O}_2 + \text{N}_2$, which we have measured over the temperature range 267 – 1100 K. We have also studied the reaction $\text{Li} + \text{O}_2 + \text{He}$ from $T = 267$ to 1000 K. Kramer et al.²⁶ obtained the result $k_1(T = 463 \text{ K}, \text{M} = \text{He}) = 2.1 \times 10^{-30} \text{ cm}^6 \text{ molecule}^{-2} \text{ s}^{-1}$, about a factor of 2 greater than our result between 400 and 500 K (Table I). This comparison is illustrated in Figure 5, along with a measurement by Kramer et al.²⁶ of $k_1(\text{M} = \text{Ar}, T = 390 \text{ K}) = 6.3 \times 10^{-30} \text{ cm}^6 \text{ molecule}^{-2} \text{ s}^{-1}$. The rate coefficients of termolecular reactions with Ar as the third body are usually slightly slower than the analogous reactions with N_2 as the third body.³⁴ This was certainly found to be the case in a study by Silver et al.²⁶ of the analogous recombination reactions between Na or K atoms with O_2 in the presence of Ar or N_2 . In the present case, however, the result of Kramer et al.²⁷ with $\text{M} = \text{Ar}$ is roughly twice as fast as our measurement of $k_1(T = 400 \text{ K}, \text{M} = \text{N}_2)$ (Table I and Figure 5).

Thus, the results of Kramer et al.²⁶ for both $\text{M} = \text{He}$ and Ar are faster by about a factor of 2 than the present study for $\text{M} = \text{He}$ and N_2 , respectively. Kramer et al.²⁶ used the resonance ionization spectroscopy technique to probe the Li atom concentration following the pulsed photolysis of LiI vapor entrained from a heated stainless steel cup. Those workers did not describe any evidence of I_2 production arising from the heterogeneous reaction 3 which should have been present to some extent in their experimental arrangement where a stream of O_2 in the bath gas was actually passed over the cup containing a sample of LiI heated to about 570 K. (See the discussion above.) The degree to which the production of I_2 in their system²⁶ would remain consistent with

their observed third-order kinetic behavior and hence lead to an overestimation of the rate constant is difficult to determine since no details are provided of the flow rates or of the manner in which the total pressure in their reactor was adjusted.

The values of $k_1(T)$ for $M = N_2$ and He measured in this study are close to those determined previously for the analogous reactions of Na and K atoms with O₂ in the presence of these two third bodies.^{5,22,23} The small negative temperature dependencies of $k_1(T)$ for both third bodies, indicated in expression 4, are also in accord with those found for the analogous reactions for Na and K.^{5,22,23} Note that the temperature dependence for reaction 1 with $M = He$ is smaller than that with $M = N_2$, so that the ratio of the rate coefficients for the third bodies decreases with temperature: $k_1(M = N_2)/k_1(M = He) = 3.7$ when $T = 267$ K; at $T = 1000$ K, $k_1(M = N_2)/k_1(M = He) = 1.3$. This convergence in rate coefficients is illustrated in Figures 4 and 5. The relative increase with temperature of the collision efficiency of He as a third body, when compared to a third body such as N₂, has been observed in collisional-energy-transfer studies of other small molecules.^{34,36}

We now describe an extrapolation of the measured rate data on Li + O₂ + M from the experimental temperature range of 267–1100 K down to temperatures found in the mesosphere and to typical flame temperatures above 1500 K.

Extrapolation of $k_1(Li + O_2 + M)$ from 140 to 2200 K. The role of the energy-transfer and atom-chaperon mechanisms in reaction 1 has been discussed by Kramer et al.²⁶ In the case of $M = Ar$, they proposed that the long-range interaction between Li and Ar,³⁵ which is slightly greater than that between Li and O₂,³⁵ results in reaction 1 proceeding by the atom-chaperon mechanism as well as by energy transfer to the third body. From their experimental data over a large range in Ar pressures it was deduced²⁶ that the atom-chaperon route might account for about 20% of the reaction at $T = 390$ K. By contrast, reaction 1 with $M = He$ appeared to proceed only by energy transfer, as expected in view of the small interaction between Li and He.³⁵ Margoliash and Meath³⁵ have also shown that the van der Waals interaction between Li and N₂ is of the same order as that between Li and O₂, so that a similar minor contribution from the atom-chaperon mechanism to the overall rate may be present when N₂ is the third body. For the purpose of this calculation we assume that reaction 1 goes primarily by the energy-transfer mechanism.

It is also necessary to establish to what extent the experimental measurements of $k_1(T)$ in this study have been made below the low-pressure limit of the termolecular reaction. We invoke a method for determining the falloff of reaction 1 derived by Luther and Troe³⁷ and Troe,³⁸ which has subsequently been adopted by NASA as a standard procedure.³⁹ The second-order rate coefficient k_{rec} in the falloff region of the reaction is given by

$$k_{rec} = \frac{k_{rec,\infty}k_{rec,0}[M]F}{k_{rec,\infty} + k_{rec,0}[M]} (1 + [\log(k_{rec,0}[M]/k_{rec,\infty})^2]^{-1}) \quad (5)$$

where $k_{rec,0}$ and $k_{rec,\infty}$ are the rate coefficients at the low-pressure and high-pressure limits, respectively. F is the broadening factor first introduced in the original Lindemann–Hinshelwood expression to describe the form of the falloff from $k_{rec,0}$ to $k_{rec,\infty}$, and for which an improved but relatively simple form was derived by Luther and Troe³⁷ in terms of RRKM theory. We adopt the suggested value for small molecules near room temperature of 0.6–0.7.^{38,39} $k_{rec,\infty}$ may be estimated in terms of the orbiting criteria on the attractive surface due to the long-range van der Waals interaction between Li and O₂⁴⁰

$$k_{rec,\infty} = \pi(2C_6/RT)^{1/3}(8RT/\pi\mu)^{1/2}\Gamma(2/3) \quad (6)$$

where $C_6 = 161 \pm 2$ hartree bohr⁶,³⁵ and μ is the reduced mass of the collision. This yields $k_{rec,\infty}(T = 267 \text{ K}) = 2.7 \times 10^{-10} \text{ cm}^3 \text{ molecule}^{-1} \text{ s}^{-1}$. A numerical solution of eq 5 at the highest pressure (15 Torr of N₂) at which reaction 1 was studied at $T = 267$ K indicates that $k_1/k_{rec,0} = 0.92$ –0.97, so that our experiments are essentially at the low-pressure limit. A similar result was obtained by Silver et al.²³ from an analysis of their experimental work on the analogous reactions of Na and K.

In order to carry out a temperature extrapolation of $k_1(T)$, we employ the formalism of Troe^{38,41} which again is based on a simplified form of RRKM theory. The calculation proceeds by determining the strong collision rate constant for the reverse unimolecular decomposition reaction in the low-pressure limit, k_0^{sc} . The rate constant for the strong collision recombination reaction is then derived by detailed balancing through the equilibrium constant:⁴¹

$$k_{rec,0}^{sc} = K_{eq}k_0^{sc} \quad (7)$$

$k_{rec,0}$ is then expressed as a product of the strong collision rate constant $k_{rec,0}^{sc}$ and a weak collision efficiency, β_c , for the energy transfer

$$k_{rec,0} = \beta_c k_{rec,0}^{sc} \quad (8)$$

where β_c lies between 0 and 1 and is generally obtained by comparing $k_{rec,0}^{sc}$ with experiment. The temperature dependence of β_c is given by

$$\frac{\beta_c}{1 - \beta_c^{1/2}} = \frac{-\langle \Delta E \rangle}{F_E RT} \quad (9)$$

where $\langle \Delta E \rangle$ is the average energy transferred per collision; this quantity may be determined through eq 9 if β_c is known at a particular temperature. In the case of N₂ or He as third bodies, $\langle \Delta E \rangle$ has generally been found to be proportional to T^n where $0 < n < 1$.^{34,36,42}

The strong collision rate constant for the unimolecular dissociation reaction may be expressed as⁴¹

$$k_0^{sc} = \frac{Z_{LJ}\rho(E_0)RT \exp(-E_0/RT)F_E F_{anh} F_{rot} F_{corr}}{Q_{vib}} \quad (10)$$

where Z_{LJ} is the Lennard-Jones reference collision frequency between LiO₂ and M; $\rho(E_0)$ is the density of states of LiO₂ at the critical energy, E_0 ; F_E , F_{anh} , and F_{rot} are correction terms arising from the energy dependence of the density of states, from the vibrational anharmonicity of LiO₂, and from rotational contribution to the density of states.⁴¹ F_{corr} is a correction factor to account for the coupling between different degrees of freedom and is usually taken as unity. Q_{vib} is the vibrational partition function. Z_{LJ} is calculated in terms of the appropriate collision diameter and reduced collision integral.⁴¹

The calculation of F_{rot} represents a major source of uncertainty in the calculation of k_0^{sc} from eq 10.³⁸ Following our earlier procedure⁵ and that of Husain et al.,²² we have employed the improvement suggested by Troe³⁸ for calculating F_{rot} at low temperatures by replacing the van der Waals potential with a Morse potential to describe the breaking of the Li–O₂ bond, combined with a polyatomic model of the centrifugal barrier.³⁸

Data Input for Calculations. The parameters used in the application of the Troe formalism⁴¹ are listed in Table II. The choice of parameters is discussed below.

(1) *Lennard-Jones Parameters.* $\sigma(\text{LiO}_2)$ and $\epsilon(\text{LiO}_2)$ have to be assumed. We have set them equal to estimates for the corresponding parameters describing LiOH which we derived previously.³ The Lennard-Jones model is not a good description of the intermolecular forces involving a highly polar molecule like

(35) Margoliash, D. J.; Meath, W. J. *J. Chem. Phys.* **1978**, *68*, 1429.

(36) Heymann, M.; Hippler, H.; Troe, J. *J. Chem. Phys.* **1984**, *80*, 1853.

(37) Luther, K.; Troe, J. In *Proceedings of the 17th International Symposium on Combustion*; The Combustion Institute: Pittsburgh, PA, 1978; p 535.

(38) Troe, J. *J. Phys. Chem.* **1979**, *83*, 114.

(39) "Chemical Kinetics and Photochemical Data for Use in Stratospheric Modeling: Evaluation Number 7", JPL/NASA Publication 85-37, 1985.

(40) Smith, I. W. M. *Kinetics and Dynamics of Elementary Gas Reactions*; Butterworths: London, 1980.

(41) Troe, J. *J. Chem. Phys.* **1977**, *66*, 4745, 4758.

(42) Heymann, M.; Hippler, H.; Plach, H. J.; Troe, J. *J. Chem. Phys.* **1987**, *87*, 3867.

TABLE II: Extrapolation of Rate Data for the Reaction $\text{Li} + \text{O}_2 + \text{M}^a$

Input Parameters for the LiO_2 Molecule	
$R_{\text{Li-O}} = 1.77 \text{ \AA}$, $R_{\text{O-O}} = 1.33 \text{ \AA}$, $I_{\text{ABC}} = 7.71 \times 10^3 \text{ amu}^3 \text{ \AA}^6$	
$\nu_1 = 698.8 \text{ cm}^{-1}$, $\nu_2 = 494.4 \text{ cm}^{-1}$, $\nu_3 = 1096.9 \text{ cm}^{-1}$,	
$E_0 = 240 \text{ kJ mol}^{-1}$	
$\sigma(\text{LiO}_2) = 3.5 \text{ \AA}$, $\epsilon(\text{LiO}_2)/k = 2240 \text{ K}$	
Data for $\text{Li} + \text{O}_2 + \text{M}$ at $T = 267 \text{ K}$	
$\sigma(\text{LiO}_2\text{-N}_2) = 4.3 \text{ \AA}$, $\epsilon(\text{LiO}_2\text{-N}_2)/k = 450 \text{ K}$, $Z_{\text{LJ}} = 6.8 \times 10^{-10} \text{ cm}^3 \text{ molecule}^{-1} \text{ s}^{-1}$	
$\sigma(\text{LiO}_2\text{-He}) = 3.1 \text{ \AA}$, $\epsilon(\text{LiO}_2\text{-He})/k = 150 \text{ K}$, $Z_{\text{LJ}} = 4.8 \times 10^{-10} \text{ cm}^3 \text{ molecule}^{-1} \text{ s}^{-1}$	
$K_{\text{eq}} = 1.34 \times 10^{23} \text{ cm}^3 \text{ molecule}^{-1}$	
$s = 3$, $m = 2$, $r = 0$, $Q_{\text{vib}} = 1.10$, $a = 0.992$, $\rho(E_0) = 0.0495$, $F_E = 1.018$	
$F_{\text{anh}} = 1.72$, $F_{\text{rot}} = 45.78$, $I^+/I = 58.27$, $C_r = 0.0134$,	
$\nu = 1.446$, $k_{\text{rec},0} = 8.0 \times 10^{-30} \text{ cm}^6 \text{ molecule}^{-2} \text{ s}^{-1}$	
$\beta_c(\text{M} = \text{N}_2) = 0.61$, $\langle \Delta E \rangle(\text{M} = \text{N}_2) = -6.16 \text{ kJ mol}^{-1}$	
$\beta_c(\text{M} = \text{He}) = 0.23$, $\langle \Delta E \rangle(\text{M} = \text{He}) = -1.01 \text{ kJ mol}^{-1}$	

^a For definition of symbols not in the present text, see ref 38 and 41.

$\text{Li} + \text{O}_2^{-1,2,43}$ However, the polarizability of He is so small⁴³ that it probably serves as a useful reference frequency; in this case we employ the standard combination rules⁴³ to derive the parameters which are listed in Table II. In the case of collisions between LiO_2 and N_2 , we have increased $\sigma(\text{LiO}_2\text{-N}_2)$ by an arbitrary 20% above the value obtained from application of the combination rules.⁴³ This results in a better fit to the experimental data and is in accord with the greater long-range force to be expected between the significant dipole moment of LiO_2 ^{1,2} and the more polarizable N_2 .⁴³

(2) *Fundamental Frequencies and Dissociation Energy of LiO_2 .* The bond lengths and vibrational frequencies listed in Table II are taken from the study by Andrews and co-workers¹ of LiO_2 in an inert gas matrix and are assumed to be the same in the gas phase. The vibrational frequency ν_3 corresponds to the O_2^- stretching frequency. The bond energy of LiO_2 has been estimated by Alexander² to be about 220 kJ mol^{-1} and by Dougherty et al.⁴⁴ from flame photometric measurements to be $222 \pm 25 \text{ kJ mol}^{-1}$. Both of these estimates are subject to large uncertainties.^{1,44} We have chosen $E_0 = 240 \text{ kJ mol}^{-1}$, which gives a better fit to our experimental data.

The results of applying the Troe formalism⁴¹ to reaction 1 are listed in Table I for both $\text{M} = \text{N}_2$ and He at $T = 267 \text{ K}$. The values of $\beta_c(\text{M} = \text{N}_2) = 0.61$ and $\beta_c(\text{M} = \text{He}) = 0.23$ are obtained by comparing $k_{\text{rec},0}^{\text{sc}}$ with the result for $k_1(T = 267 \text{ K})$ from the best fit to the experimental data given in expression 4. The values of β_c and $\langle \Delta E \rangle$ are in accord with a wide body of data on the collision efficiencies of these two third bodies.^{5,34,36,37,41}

(43) Hirschfelder, J. O.; Curtiss, C. F.; Bird, R. B. *Molecular Theory of Gases and Liquids*; Wiley: New York, 1958.

(44) Dougherty, G. J.; McEwan, M. J.; Phillips, L. F. *Combust. Flame* **1973**, *21*, 253.

The fit of the Troe formalism to the experimental data at $T = 267 \text{ K}$ can now be used to calculate $k_{\text{rec},0}$ over the temperature range of the present study and to compare with the experimental values of $k_1(T)$. The best fit to both sets of data is obtained with $\langle \Delta E \rangle \propto T^{0.3}$ for N_2 and $\langle \Delta E \rangle \propto T^{1.3}$ for He; the temperature dependence of $\langle \Delta E \rangle$ for $\text{M} = \text{N}_2$ is very close to a result from recent work on collisional energy transfer from vibrationally excited CS_2 ⁴² while that for He is somewhat higher than has been observed from such experiments.⁴² These fitted calculations are illustrated in Figure 5 and are seen to be highly satisfactory. Patrick and Golden⁴⁵ have previously calculated $k_1(200 \text{ K} < T < 2000 \text{ K}, \text{M} = \text{N}_2)$ using the Troe formalism⁴¹ but had to assume values for β_c and $\langle \Delta E \rangle$ in the absence of any experimental data. There is reasonable agreement (within 40%) near and below room temperature between their calculation and the present one; between 500 and 2000 K the calculated values of $k_1(T)$ from their study are about a factor of 2 smaller.

Values of $k_1(T)$ can now be calculated outside the experimental region between 267 and 1100 K and are plotted in Figure 5 between 150 and 2000 K. Notice that the reaction rates for $\text{M} = \text{N}_2$ and He become equal close to $T = 2000 \text{ K}$. The recommended result from the present study for $k_1(\text{Li} + \text{O}_2 + \text{N}_2)$ in the temperature region of interest for modeling the mesospheric chemistry of Li is given by

$$k_1(140 \text{ K} < T < 240 \text{ K}) = 6.3 \times 10^{-30} (T/200 \text{ K})^{-0.93} \text{ cm}^6 \text{ molecule}^{-2} \text{ s}^{-1}$$

The extrapolation of $k_1(\text{Li} + \text{O}_2 + \text{N}_2)$ to flame temperatures yields the following result:

$$k_1(1500 \text{ K} < T < 2200 \text{ K}) = 3.7 \times 10^{-31} (T/2000 \text{ K})^{-1.72} \text{ cm}^6 \text{ molecule}^{-2} \text{ s}^{-1}$$

The values of $k_1(\text{Li} + \text{O}_2 + \text{M})$ lie between those of the analogous reactions of Na and K at the same temperatures, with $k(\text{K} + \text{O}_2 + \text{N}_2)$ being fastest.^{5,22,23} This observation can be understood in terms of RRKM theory.^{41,45} On the one hand, the Li-O₂ bond energy^{2,44} is greater than that of Na-O₂^{5,24,25} or K-O₂,^{22,24} and this leads to a larger value for k_1 than the recombination rate constant for $\text{Na} + \text{O}_2 + \text{M}$. On the other hand, the vibrational frequencies of KO_2 are much lower than those of LiO_2 ; this is manifest in a much higher density of vibrational states at the critical energy for KO_2 ²² and on balance leads to a faster rate constant for $\text{K} + \text{O}_2 + \text{M}$ than k_1 .^{41,45}

Acknowledgment. This work was supported under Grant ATM-8616338 from the National Science Foundation. We thank Dr. Paul Marshall (Rensselaer Polytechnic Institute) for a computer implementation of the Troe formalism.

Registry No. Li, 7439-93-2; O_2 , 7782-44-7; N_2 , 7727-37-9; He, 7440-59-7.

(45) Patrick, R.; Golden, D. M. *Int. J. Chem. Kinet.* **1984**, *16*, 1567.